Structural Versatility of Peptides from $C^{\alpha,\alpha}$-Dialkylated Glycines. A Conformational Energy Computation and X-ray Diffraction Study of Homopeptides from 1-Aminocyclohexane-1-carboxylic Acid[1]

V. Pavone, E. Benedetti,* V. Barone, B. Di Blasio, F. Lelj, C. Pedone, and A. Santini

Department of Chemistry, University of Naples, 80134 Naples, Italy

M. Crisma, G. M. Bonora, and C. Toniolo*

Biopolymer Research Center, CNR, Department of Organic Chemistry, University of Padova, 35131 Padova, Italy. *Received April 20, 1987*

ABSTRACT: Conformational energy computations on the 1-aminocyclohexane-1-carboxylic acid monopeptide, Ac–Acc^6–NHMe, indicate that this $C^{\alpha,\alpha}$-dialkylated, cyclic α-amino acid residue is conformationally restricted and that its minimum energy conformation falls in the $\alpha/3_{10}$ helical region, irrespective of the position (either axial or equatorial) of the α-amino group. The results of the theoretical analysis are in agreement with the crystal-state structural tendency of $Z(Acc^6)_4O$-*t*-Bu (monoclinic and triclinic forms) and *p*-$BrBz(Acc^6)_4O$-*t*-Bu, determined by X-ray diffraction and also described in this paper (formation of 3_{10} helices). The implications for the use of Acc^6 residues in designing conformationally constrained analogues of bioactive peptides are briefly discussed.

Introduction

Previous investigations from our and other laboratories on the crystal-state structural preferences of peptides from $C^{\alpha,\alpha}$-dialkylated glycines have dealt with Aib (α-aminoisobutyric acid or $C^{\alpha,\alpha}$-dimethylglycine),[2-6] Deg ($C^{\alpha,\alpha}$-diethylglycine),[7] Dpg ($C^{\alpha,\alpha}$-di-*n*-propylglycine),[8] and Acc^5 (1-aminocyclopentane-1-carboxylic acid)[9] containing compounds.

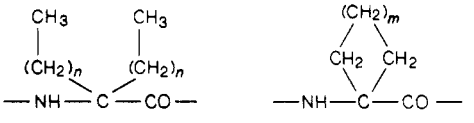

To expand the picture of the structural characteristics of peptides from $C^{\alpha,\alpha}$-dialkylated glycines, we report here are results on peptides from Acc^6 (1-aminocyclohexane-1-carboxylic acid) and, in particular, of (1) conformational energy computations of the monopeptide Ac–Acc^6–NHMe (Ac, acetyl; NHMe, methylamino) as a function of the relevant N–C^{α}–C′ (τ) bond angle and the position (either axial or equatorial) of the α-amino group and (2) X-ray diffraction analyses of the two N- and C-blocked homotetrapeptides $Z(Acc^6)_4O$-*t*-Bu (Z, benzyloxycarbonyl; O-*t*-Bu, *tert*-butoxy), in the monoclinic and in the triclinic form as well, and *p*-$BrBz(Acc^6)_4O$-*t*-Bu (*p*-BrBz, *p*-bromobenzoyl).

This study was expected to provide information on the structural effect induced by Acc^6 residues when incorporated into analogues of bioactive peptides. To our knowledge, Acc^6-containing peptides synthesized so far range from analogues of the formyl–methionyl chemoattractant[10] to the sweetening agent aspartame[11-13] and from angiotensin II[14] to enkephalins[15] and the antitumor and antiviral agents 2,5-piperazinediones.[16] In addition, the still unavailable information on the preferred conformation of the homopolymer was also considered an interesting motivation for this study. Actually, poly$(Acc^6)_n$ was prepared by two groups[17,18] (either by the *N*-carboxy anhydride[17] or by the oxazolone[18] method), but its structural properties were not investigated.

The results of our analysis of the solution-preferred conformation of the complete N- and C-protected Acc^6 homopeptides series from monomer to pentamer by infrared absorption and ^1H nuclear magnetic resonance are reported in the following paper.[19] Preliminary communications of part of these data have been presented.[20,21] X-ray diffraction structures of H–Acc^6–OH hydrochloride,[22] a few derivatives,[1] and peptides shorter than tetramers[1,23,24] have been published.

Experimental Section

Synthesis of Peptides. The synthesis and characterization of the two Acc^6 homotetrapeptides, $Z(Acc^6)_4O$-*t*-Bu and *p*-$BrBz(Acc^6)_4O$-*t*-Bu, are described in the following paper.[19]

Conformational Energy Computations. The geometries of the acetamido and methylamido blocking groups were those proposed by Scheraga and co-workers.[25,26] Conformational energy computations were performed by using the package NB/83, which evaluates the conformational energy as a sum of nonbonded, electrostatic, and H-bond contributions, as suggested by Momany et al.[25] and taking into account the recent updating of Némethy et al.[26] Consistent with this procedure, atomic charges for the electrostatic contributions were obtained from CNDO/2 computations. The conformational space was mapped by calculating the conformational energy at 10° intervals for the torsion angles φ and ψ, with the ω angles fixed at 180° and the terminal methyl groups frozen into staggered conformations.[27] Minimum energy conformations were obtained in all the low-energy regions located in the above search, minimizing the energy with respect to all torsion angles by the OPT/83 package[28] using Davidon–Fletcher–Powell[29,30] and Newton–Raphson[31] algorithms. Conformational energies are expressed as $\Delta E = E - E_0$, where E_0 is the energy of the most stable conformation. All computations were performed on the VAX 11/750 computer of the Chemistry Department at the University of Naples.

X-ray Diffraction. Preliminary oscillation and Weissenberg photographs were taken to establish the crystal symmetry and the space group. Determination of the cell constants and collection of the X-ray intensity data were performed on a CAD4 Enraf-Nonius diffractometer of the Centro Interdipartimentale di Metodologie Chimico-Fisiche at the University of Naples, equipped with PDP8/E and PDP11/34 Digital computers. For the structure determination and refinement, the SDP package (structure determination program) was used. Unit cell parameters were obtained by a least-squares procedure on the angular pa-

0024-9297/88/2221-2064$01.50/0

Table I
Crystallographic Data for Z(Acc^6)$_4$O-*t*-Bu (Monoclinic and Triclinic Forms) and *p*-BrBz(Acc^6)$_4$O-*t*-Bu

parameter	Z(Acc^6)$_4$-O-*t*-Bu	Z(Acc^6)$_4$-O-*t*-Bu	*p*-BrBz-(Acc^6)$_4$O-*t*-Bu
mol formula	$C_{40}H_{60}N_4O_7$	$C_{40}H_{60}N_4O_7$	$C_{39}H_{57}N_4O_6Br$
mol wt, amu	708.95	708.95	757.82
cryst system	monoclinic	triclinic	monoclinic
space group	$P2_1/n$	$P\bar{1}$	$P2_1/n$
Z, molecules/unit cell	4	2	4
a, Å	11.779 (2)	10.599 (2)	10.675 (4)
b, Å	18.705 (3)	18.320 (3)	19.119 (7)
c, Å	18.000 (4)	11.750 (3)	19.266 (7)
α, deg	90.00	82.61 (5)	90.00
β, deg	96.83 (5)	117.46 (5)	92.88 (10)
γ, deg	90.00	97.26 (5)	90.00
V, Å^3	3937.7	2001.8	3927.1
d (calcd), g/cm^3	1.194	1.170	1.280
d (exptl), g/cm^3	1.20	1.17	1.28
radiation, Å	Cu Kα, 1.5418	Cu Kα, 1.5418	Cu Kα, 1.5418
no. of indep refls	7462	7577	7430
refls with $I \geq 3\sigma(I)$	6047	4431	5085
final R value	0.066	0.081	0.079
final weighted R value	0.074	0.082	0.089
esd of an observation of unit weight	1.758	1.409	1.887
temp	ambient	ambient	ambient
crystallizatn solvent	$(CH_3)_2CO$	$(CH_3)_2CO$	$(CH_3)_2CO$

rameters of 25 high-angle reflections. The analysis of the peak profiles suggested an ω–2θ scan mode with a scan angle equal to $(1.0 + 0.15 \tan\theta)°$; background counts were taken in an additional area of $\Delta\omega/4$ on both sides of the main scan with the same scan speed for each reflection. A crystal-to-counter distance of 368 mm was used with counter entrance aperture of 4 mm.

The tube placed between the goniometer head, and the detector was evacuated. Prescan runs were made at a speed of 3.5°/min. Reflections with a net intensity $I < 0.5\sigma(I)$ were flagged as "weak"; those having $I \geq 0.5\sigma(I)$ were measured at slower speeds (1.0–3.5°/min) depending on the value of $\sigma(I)/I$. Two intensity control reflections were measured every 60 min of X-ray exposure time to monitor the crystal and the electronic stability; no significant change in intensity was observed during data collection. Orientation matrix checks were made with respect to the scattering vectors of four well-centered reflections every 200 measured reflections; reorientation was made by using 25 high-angle reflections, if the displacements of the measured scattering vector exceeded the calculated value of 0.15°. The total number of independent reflections and those used in the refinement [$I \geq 3\sigma(I)$] are given in Table I. All reflections were corrected for Lorentz and polarization effects.

The structures were solved by means of direct methods, with use of MULTAN,[32] with the exception of *p*-BrBz(Acc^6)$_4$O-*t*-Bu, which was solved by using Patterson vector analysis. The structures were refined by a full-matrix least-squares procedure, minimizing the quantity $\sum w(F_o^2 - F_c^2)^2$ with weights w equal to $1/\sigma(F_o^2)$. The equation used to calculate $\sigma(F_o^2)$ is the following:

$$\sigma(F_o^2) = (20.1166(\mathrm{ATN}/\mathrm{NPI})(C + R^2B)^{1/2})/Lp$$

where ATN is the attenuation factor, NPI is the ratio of the fastest possible scan rate to scan rate for the reflection, C is the total count, R is the ratio of scan time to background counting time, B is the total background count, and Lp are the Lorentz and polarization factors.

All heavy atoms were refined with anisotropic temperature factors. Hydrogen atoms were introduced in their stereochemically expected positions with isotropic temperature factors equal to the equivalent B factor of the atom to which each of them is linked.

Refinements were ended when the shifts in the atomic coordinates and anisotropic temperature factors for the heavy atoms were less than $^1/_5$ and $^1/_3$ of the corresponding standard deviations, respectively. The atomic scattering factors, with the real and imaginary dispersion corrections, for all atomic species were calculated according to Cromer and Waber.[33] Crystallographic data for the three structures are reported in Table I. Tables of final atomic parameters for all nonhydrogen atoms for the three structures have been deposited and are available from the Cambridge Crystallographic Data Center.

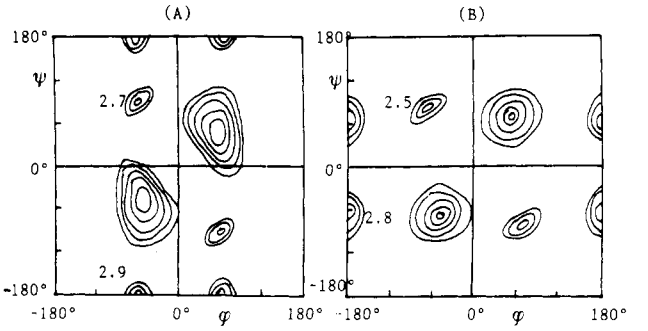

Figure 1. Conformational energy contour map for Ac–Acc^6–NHMe for (A) axial and (B) equatorial placements of the –NH group. The contour lines are spaced 1 kcal/mol up to 5 kcal/mol over the 10° grid point of lowest energy for each map, located at $(\varphi, \psi) = (\pm 60°, \pm 30°)$ in map A and at $(\varphi, \psi) = (\pm 40°, \pm 80°)$ in map B.

Results and Discussion

Conformational Energy Computations. Figure 1 gives the conformational energy map for the monopeptide Ac–Acc^6–NHMe, with –NH in the axial position (case A) or in the equatorial position (case B), respectively. Compared to the monopeptides of C$^\alpha$-monoalkylated α-amino acids, both maps show a drastic reduction of the accessible (φ, ψ) space. The two maps are very similar, showing in practice an almost blocked value for one torsion angle and a larger conformational freedom for the other; in fact, larger freedom is observed for ψ when the –NH group is in an axial position, while the –NH group in an equatorial position produces a larger freedom in the φ angle. The most stable conformations fall in both cases in the $\alpha/3_{10}$ helical region ($\varphi \approx \pm 70°$, $\psi \approx \pm 30°$ in case A and $\varphi \approx \pm 40°$, $\psi \approx \pm 80°$ in case B).

Additional minima, ≈3.0 kcal/mol higher in energy, are observed for (i) C_7 structures (3→1 H-bonded conformations) with $\varphi \approx \pm 70°$, $\psi \approx \mp 70°$ in case A and $\varphi \approx \pm 60°$, $\psi \approx \mp 80°$ in case B and (ii) quasiextended conformations ($\varphi = \pm 70°$, $\psi = 180°$ in case A and $\varphi = 180°$, $\psi = \pm 60°$ in case B). Although this kind of computation cannot give reliable values for the relative stabilities of the two conformations, it is noteworthy that the axial placement of the –NH group results in a lower total energy, in agreement with the more frequent occurrence of this conformation (see below). From geometry optimization a τ bond angle greater than the tetrahedral value (≈112°) is obtained. The energy difference between the different energy minima remains practically unchanged after geometry optimization, and also the φ and ψ values are not significantly modified. However, in all the conformations the ω_0 torsion angle is reduced to ≈176°.

X-ray Diffraction Analyses. We have determined the molecular and crystal structures of the two N- and C-blocked Acc^6 homotetrapeptides, namely, Z(Acc^6)$_4$O-*t*-Bu (monoclinic and triclinic forms) and *p*-BrBz(Acc^6)$_4$O-*t*-Bu. The three X-ray molecular structures with the atomic numbering for the atoms of the peptide skeleton are shown in Figures 2–4, respectively. Figure 5 describes the average geometry for an Acc^6 residue as derived from a statistical analysis of the structures presented in this paper. Bond lengths and bond angles are given in Table II. Torsion angles for the Acc^6 residues and the geometry of the intra- and intermolecular H bonds are given in Tables III and IV, respectively. The modes of packing of the molecules in the crystals are illustrated in Figures 6–8.

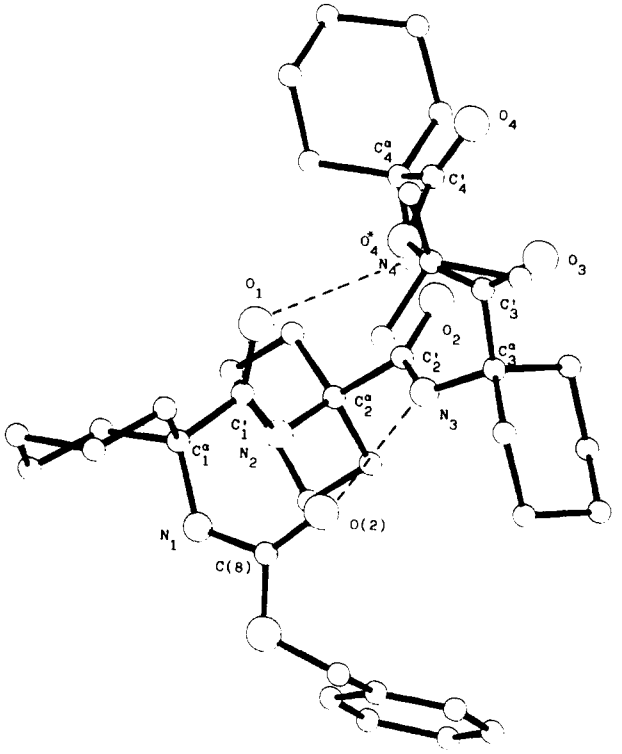

Figure 2. Molecular structure of Z(Acc^6)$_4$O-*t*-Bu (monoclinic form). The intramolecular H bonds are represented as dashed lines.

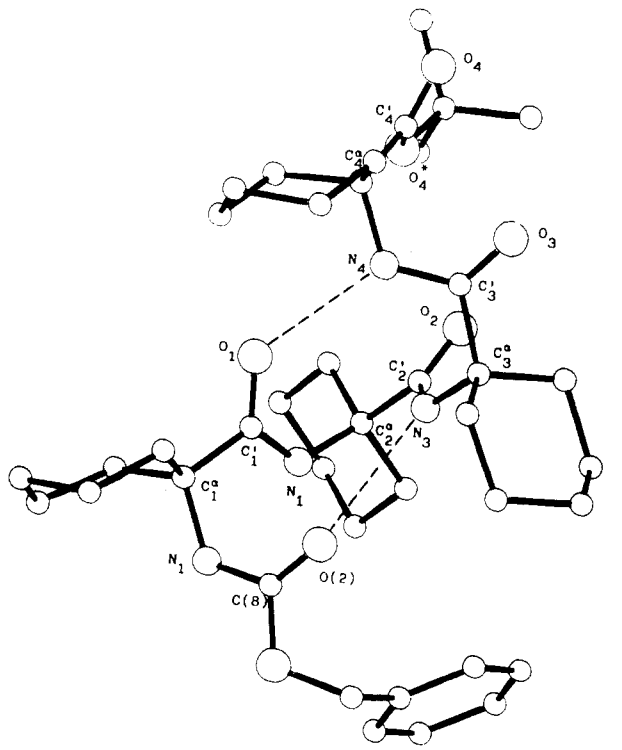

Figure 3. Molecular structure of Z(Acc^6)$_4$O-*t*-Bu (triclinic form). The intramolecular H bonds are represented as dashed lines.

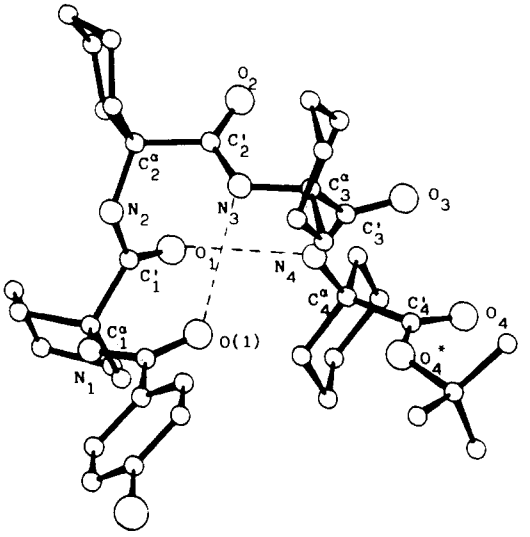

Figure 4. Molecular structure of *p*-BrBz(Acc^6)$_4$O-*t*-Bu. The intramolecular H bonds are represented as dashed lines.

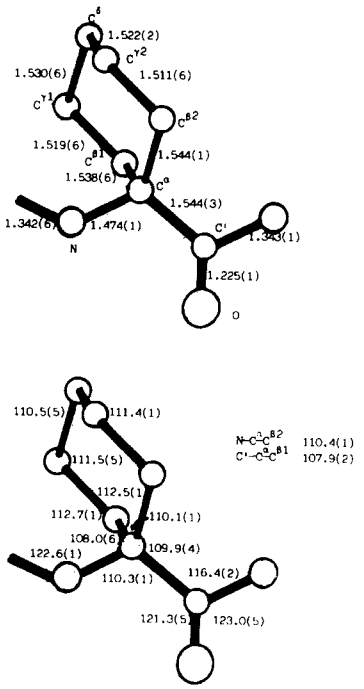

Figure 5. Average geometry for an Acc^6 residue (bond lengths, upper; bond angles, lower) derived from an analysis of the crystal structures discussed in this work.

Backbone Conformation. The succession of similar pairs of φ, ψ values[34] along the chains of Z(Acc^6)$_4$O-*t*-Bu (monoclinic form and triclinic form as well) and *p*-BrBz-(Acc^6)$_4$O-*t*-Bu generates an incipient helical structure, which can be described as a 3_{10} helix, reasonably close to the ideal case, (φ, ψ) = (±60°, ±30°).[35-37] In all three structures there are two successive intramolecular N–H···O=C H bonds of the C_{10}-III (or C_{10}-III') type.[38-40] The range of observed N···O distances for the 4→1 H bonds is 3.006–3.184 Å, within the limits expected for N–H···O–C intramolecular H bonds.[41,42] α-Helical structures, although having pairs of φ, ψ angles (±55°, ±45°) near those of the 3_{10} helices, are not compatible with the observed H-bonding schemes, being characterized by 5→1 (C_{13}) intramolecular H-bonded forms.[36,37,39] The deviations of the ω angles from the ideal value of the trans planar peptide unit (180°)[43,44] are more significant for the *p*-BrBz-protected homotetrapeptide. Also the fourth Acc^6 residue in the structures of Z(Acc^6)$_4$O-*t*-Bu (monoclinic form) and *p*-BrBz(Acc^6)$_4$O-*t*-Bu adopts a conformation in the helical region, but it has an handedness opposite to that of the preceding residues. This feature has been consistently

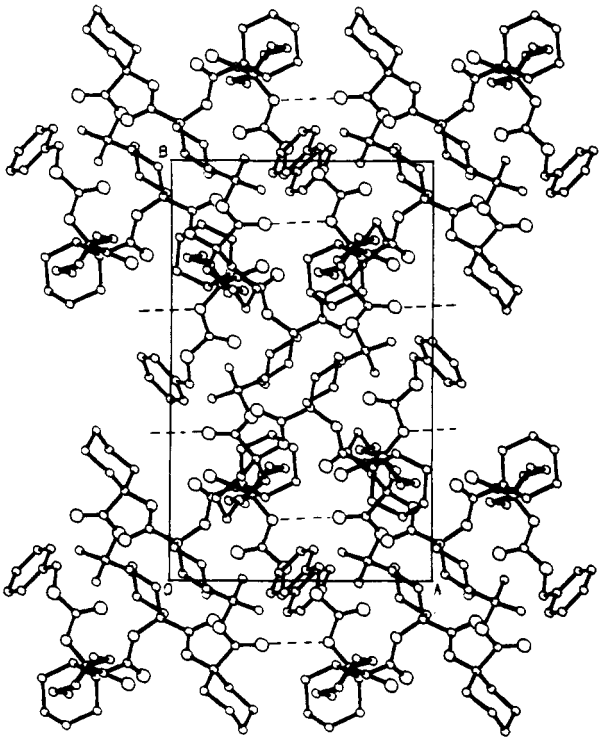

Figure 6. Mode of packing of the Z(Acc^6)$_4$O-*t*-Bu molecules (monoclinic form) projected down the *c* axis.

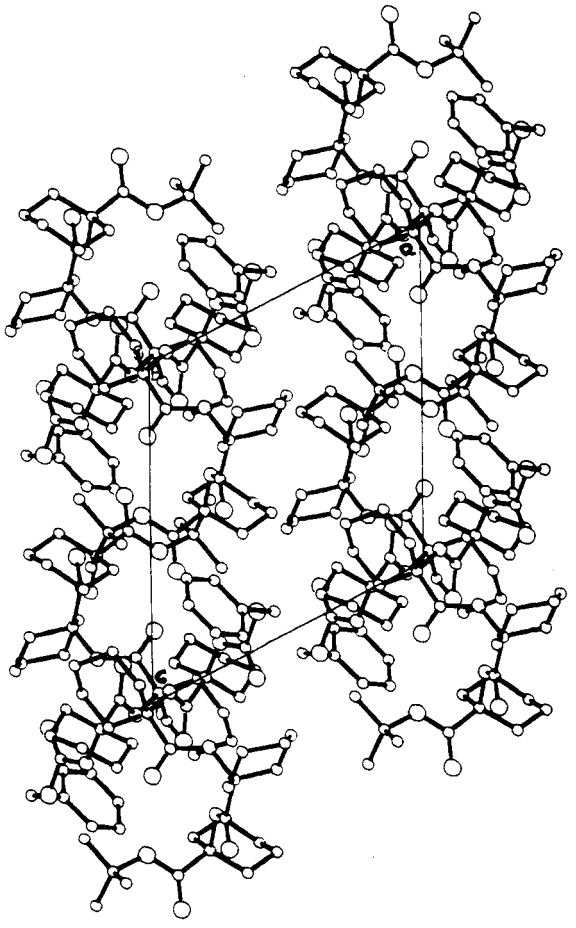

Figure 7. Mode of packing of the Z(Acc^6)$_4$O-*t*-Bu molecules (triclinic form) projected down the *b* axis.

observed in the 3_{10} helical structures formed by Aib homopeptides[2,3,45-47] and *t*-Boc(Acc^6)$_3$OMe (*t*-Boc, *tert*-butyloxycarbonyl; OMe, methoxy).[24] However, this observation (different screw sense of the last helical residue) does not hold for Z(Acc^6)$_4$O-*t*-Bu (triclinic form). This characteristic represents the main conformational difference between the two crystal forms of this homotetrapeptide. It may also be concluded that the influence of different N$^\alpha$-blocking groups on the type of helical structure and intramolecular H-bonding scheme adopted by the Acc^6 homotetrapeptides is negligible, as already found for Aib homopeptides.[2,3,45-47]

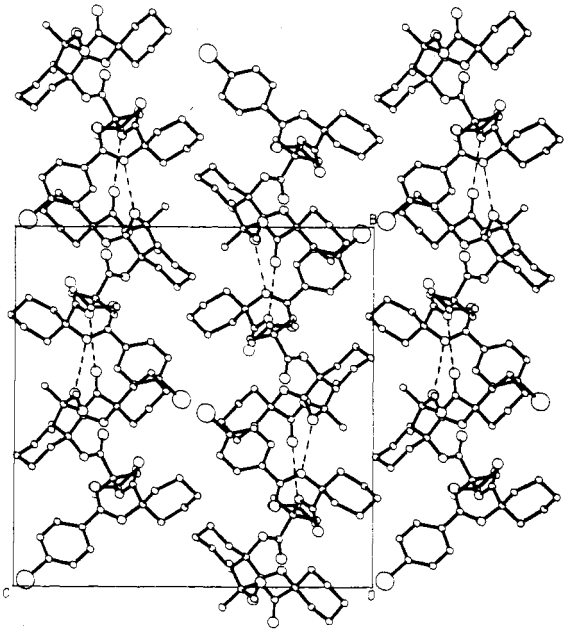

Figure 8. Mode of packing of the *p*-BrBz(Acc^6)$_4$O-*t*-Bu molecules projected down the *a* axis.

Geometry and Conformation of N- and C-Terminal Groups. The observed bond lengths and bond angles in the three structures (Table II) compare well with previously reported results for the geometry of the Z urethane,[48] *p*-BrBz amide,[1,3] and *tert*-butyl ester[2,3] groups. In particular, the decrease of the bond angle at C(8) of the Z groups N1–C(8)–O(1) by about 7°, as compared with the corresponding bond angle at C′ in the peptide group,[43,44] must be ascribed to the reduced repulsion between the O(1) atom and the nearest substituent on the N atom in urethane, compared with the corresponding repulsion involving the C$^\alpha$ atom of the peptide group.

The C(8)–O(1)–C(7)–C(6) and O(1)–C(7)–C(6)–C(1) torsion angles, giving the orientation of the phenyl ring relative to the urethane moiety,[48] have values of 87.8°, 84.6° and 21.3°, 53.5°, respectively, for the two structures of the Z-protected homotetrapeptide. Interestingly, in the observed distribution of the C(8)–O(1)–C(7)–C(6) torsion angle in crystalline Z derivatives, the values are concentrated in three regions, close to 90°, −90°, and 180°, respectively; conversely, the distribution of O(1)–C(7)–C(6)–C(1) values is broad, extending over its entire range.[48] The urethane linkage is found in the usual trans conformation,[48] the corresponding ω_0 values being −168.5° and −173.6° for the two structures, respectively. This structural property, accompanied by the trans arrangement of the N(1)–C(8)–O(1)–C(7) angle (−161.5° and −161.1°), allows us to classify the Z-urethane moiety of the two structures as type b.[48-50] The ω_0 and N(1)–C(8)–O(1)–C(7) values for the *p*-BrBz group[1,3] of *p*-BrBz(Acc^6)$_4$O-*t*-Bu are −167.8° and 28.4°, respectively. The latter value indicates that the phenyl group of the *p*-BrBz moiety is slightly rotated from the amide plane.

Table II
Geometric Parameters with Estimated Standard Deviations (in Parentheses) for the Three Structures of Z(Acc^6)$_4$O-*t*-Bu (Monoclinic and Triclinic Forms) and *p*-BrBz(Acc^6)$_4$O-*t*-Bu

	Z(Acc^6)$_4$O-*t*-Bu (monoclinic)				Z(Acc^6)$_4$O-*t*Bu (triclinic)				*p*-BrBz(Acc^6)$_4$O-*t*-Bu			
	res 1	res 2	res 3	res 4	res 1	res 2	res 3	res 4	res 1	res 2	res 3	res 4
						Bond Distance[a]						
N_i–C^{α}_i	1.471 (4)	1.464 (4)	1.471 (4)	1.461 (4)	1.496 (6)	1.468 (7)	1.457 (6)	1.499 (6)	1.467 (9)	1.480 (8)	1.473 (8)	1.482 (8)
C^{α}_i–C'_i	1.543 (4)	1.547 (5)	1.527 (5)	1.543 (5)	1.544 (7)	1.536 (7)	1.577 (7)	1.522 (7)	1.550 (9)	1.549 (10)	1.547 (9)	1.541 (8)
C'_i=O_i	1.222 (4)	1.219 (4)	1.228 (4)	1.206 (4)	1.245 (5)	1.226 (6)	1.211 (5)	1.221 (4)	1.229 (8)	1.225 (8)	1.248 (7)	1.210 (7)
C'_i–N_{i+1}	1.354 (4)	1.355 (4)	1.344 (5)	1.333 (4)	1.336 (8)	1.336 (8)	1.343 (8)	1.343 (8)	1.354 (8)	1.341 (8)	1.317 (4)	1.324 (7)
C^{α}_i–$C^{\beta 1}_i$	1.536 (4)	1.539 (5)	1.540 (5)	1.544 (5)	1.516 (8)	1.552 (8)	1.520 (9)	1.546 (9)	1.542 (10)	1.542 (10)	1.539 (9)	1.540 (9)
C^{α}_i–$C^{\beta 2}_i$	1.542 (5)	1.542 (5)	1.547 (4)	1.545 (5)	1.533 (8)	1.538 (8)	1.545 (9)	1.508 (10)	1.556 (10)	1.556 (10)	1.565 (10)	1.550 (9)
$C^{\beta 1}_i$–$C^{\gamma 1}_i$	1.531 (5)	1.526 (6)	1.532 (5)	1.532 (6)	1.540 (8)	1.530 (8)	1.545 (9)	1.508 (10)	1.524 (11)	1.524 (11)	1.551 (11)	1.541 (10)
$C^{\beta 2}_i$–$C^{\gamma 2}_i$	1.524 (4)	1.537 (6)	1.528 (5)	1.530 (5)	1.535 (9)	1.508 (9)	1.548 (8)	1.506 (9)	1.511 (12)	1.511 (12)	1.529 (12)	1.518 (10)
$C^{\gamma 1}_i$–C^{δ}	1.531 (7)	1.525 (6)	1.538 (5)	1.537 (6)	1.512 (9)	1.504 (12)	1.532 (10)	1.515 (11)	1.575 (14)	1.575 (14)	1.534 (12)	1.536 (11)
$C^{\gamma 2}_i$–C^{δ}	1.520 (5)	1.524 (7)	1.522 (6)	1.524 (6)	1.507 (10)	1.530 (13)	1.509 (12)	1.538 (12)	1.526 (13)	1.526 (13)	1.500 (12)	1.521 (10)
						Bond Angle[b]						
N–C^{α}–C'	110.4 (4)	111.5 (4)	112.3 (5)	109.0 (5)	109.0 (7)	112.4 (7)	109.0 (7)	109.1 (7)	110.1 (9)	110.1 (9)	110.0 (9)	107.8 (8)
N–C^{α}–$C^{\beta 1}$	111.7 (4)	110.9 (4)	106.9 (4)	109.3 (5)	107.9 (7)	106.5 (8)	109.3 (8)	107.4 (7)	107.8 (9)	106.3 (10)	107.5 (9)	111.6 (9)
N–C^{α}–$C^{\beta 2}$	108.2 (4)	108.0 (4)	111.7 (4)	107.7 (5)	110.1 (7)	110.7 (8)	112.7 (8)	111.1 (7)	110.0 (9)	109.5 (10)	112.0 (9)	106.8 (8)
$C^{\beta 1}$–C^{α}–C'	111.2 (4)	109.1 (4)	107.9 (5)	112.5 (5)	107.5 (7)	107.6 (8)	106.4 (8)	106.6 (7)	108.2 (9)	107.7 (10)	106.0 (9)	112.0 (9)
$C^{\beta 2}$–C^{α}–C'	105.8 (4)	106.8 (4)	108.8 (5)	108.3 (5)	110.4 (8)	109.5 (8)	107.8 (8)	111.3 (9)	110.7 (10)	112.5 (12)	110.4 (9)	109.3 (8)
C^{α}–$C^{\beta 1}$–$C^{\gamma 1}$	110.5 (5)	112.4 (5)	112.3 (5)	114.5 (5)	114.4 (8)	111.3 (9)	112.6 (8)	113.3 (9)	111.4 (11)	115.2 (14)	111.6 (10)	113.2 (10)
$C^{\beta 1}$–$C^{\gamma 1}$–C^{δ}	111.9 (6)	110.7 (6)	112.0 (5)	112.0 (6)	112.7 (9)	112.3 (10)	111.1 (9)	111.7 (10)	109.3 (12)	112.8 (18)	111.7 (11)	111.5 (10)
$C^{\gamma 1}$–C^{δ}–$C^{\gamma 2}$	110.3 (6)	110.3 (7)	110.7 (6)	111.0 (6)	111.9 (10)	110.3 (11)	109.7 (10)	109.8 (11)	112.2 (3)	108.7 (9)	111.1 (12)	110.4 (10)
C^{δ}–$C^{\gamma 2}$–$C^{\beta 2}$	110.7 (5)	110.8 (6)	111.0 (5)	110.8 (6)	112.3 (9)	113.2 (11)	110.9 (10)	111.0 (10)	112.5 (13)	116.7 (20)	112.2 (12)	110.4 (10)
$C^{\gamma 2}$–$C^{\beta 2}$–C^{α}	113.1 (5)	112.2 (5)	111.7 (5)	112.1 (5)	110.9 (9))	111.8 (9)	110.6 (9)	113.0 (8)	115.8 (11)	119.6 (16)	110.0 (11)	111.8 (9)
$C^{\beta 1}$–C^{α}–$C^{\beta 2}$	109.5 (4)	110.4 (5)	109.0 (5)	109.9 (5)	111.8 (8)	110.0 (8)	109.5 (8)	111.1 (8)	110.0 (10)	110.5 (11)	109.8 (9)	109.3 (9)
C^{α}–C'–O	121.6 (5)	120.4 (5)	119.6 (5)	124.6 (5)	119.5 (8)	119.3 (8)	120.4 (9)	123.2 (7)	122.2 (10)	120.7 (10)	119.3 (10)	124.5 (9)
C^{α}–C'–N_{i+1}	115.0 (4)	115.6 (5)	118.3 (5)	109.7 (5)	117.2 (8)	117.8 (8)	115.7 (8)	112.3 (7)	115.9 (9)	115.5 (10)	116.8 (9)	110.3 (9)
O–C'–N_{i+1}	123.2 (5)	123.9 (5)	122.0 (6)	125.6 (6)	122.9 (8)	122.9 (9)	123.7 (9)	124.5 (7)	121.8 (10)	123.5 (11)	123.5 (10)	125.1 (10)
C'_{i-1}–N_i–C^{α}	121.4 (5)	124.2 (4)	124.7 (4)	122.8 (5)	121.2 (8)	125.8 (8)	122.9 (8)	119.2 (8)	122.3 (9)	121.6 (9)	124.1 (9)	122.6 (9)

[a] In angstroms. [b] In degrees.

Table III
Torsion Angles (Degrees) with Esd's for the Acc^6 Residues in Z(Acc^6)$_4$O-*t*-Bu (Monoclinic and Triclinic Forms) and *p*-BrBz(Acc^6)$_4$O-*t*-Bu

	(a) Z(Acc^6)$_4$O-*t*-Bu (monoclinic form)				(b) Z(Acc^6)$_4$O-*t*-Bu (triclinic form)				(c) *p*-BrBz(Acc^6)$_4$O-*t*-Bu			
angle	$i = 1$	$i = 2$	$i = 3$	$i = 4$	$i = 1$	$i = 2$	$i = 3$	$i = 4$	$i = 1$	$i = 2$	$i = 3$	$i = 4$
φ	−59.0 (5)	−55.4 (4)	−71.6 (5)	53.6 (5)	−57.7 (8)	−55.1 (8)	−59.8 (8)	−55.6 (8)	−52.6 (9)	−55.9 (9)	−69.4 (9)	43.6 (9)
ψ	−32.1 (4)	−31.7 (4)	−11.0 (5)	48.2 (5)	−29.0 (8)	−24.5 (8)	−34.6 (8)	−49.5 (7)	−51.6 (10)	−38.2 (9)	−32.4 (9)	55.1 (8)
ω	−172.5 (6)	−172.7 (6)	177.1 (6)	−175.5 (6)	−174.5 (10)	179.9 (10)	−176.3 (9)	176.9 (8)	−168.5 (12)	−174.5 (12)	−165.0 (12)	172.8 (11)
$\chi^{1,1}$	−66.9 (5)	−69.2 (5)	−66.4 (5)	−167.8 (6)	−72.4 (8)	−65.8 (9)	−69.4 (8)	−72.5 (9)	−175.7 (12)	−160.8 (17)	−67.2 (10)	−169.7 (11)
$\chi^{1,2}$	64.8 (5)	66.8 (5)	61.2 (5)	172.6 (6)	67.5 (8)	63.8 (9)	65.9 (8)	69.1 (8)	167.8 (13)	149.0 (19)	62.7 (10)	176.4 (11)
θ_1	−55.7 (5)	−55.5 (6)	−54.3 (5)	50.2 (6)	−47.9 (9)	−56.2 (10)	−55.3 (9)	−53.6 (10)	60.1 (11)	56.7 (16)	−53.8 (11)	52.6 (10)
θ_2	55.4 (5)	57.9 (6)	54.0 (5)	−53.1 (6)	50.5 (9)	55.0 (10)	56.3 (9)	57.1 (10)	−56.9 (13)	−56.9 (19)	54.0 (12)	−55.0 (10)
θ_3	−57.5 (5)	−58.5 (6)	−56.0 (5)	57.6 (6)	−55.8 (9)	−54.6 (11)	−50.8 (9)	−58.1 (10)	50.0 (12)	46.9 (18)	−57.0 (12)	58.9 (10)
θ_4	57.7 (5)	56.6 (6)	58.5 (5)	−58.8 (5)	56.7 (9)	54.8 (10)	59.5 (9)	55.7 (9)	−47.0 (12)	−37.8 (16)	58.5 (12)	−60.1 (10)
θ_5	−55.0 (5)	−53.0 (5)	−56.7 (5)	53.6 (5)	−52.5 (8)	−53.6 (9)	−56.0 (8)	−50.4 (9)	49.2 (12)	32.2 (15)	−56.6 (10)	55.6 (9)
θ_6	55.1 (5)	52.3 (5)	54.6 (5)	−49.8 (5)	48.9 (8)	54.1 (9)	54.5 (9)	49.2 (8)	−55.7 (11)	−42.0 (15)	54.9 (10)	−51.8 (10)

Table IV
Intra- and Intermolecular H Bonds in the Molecules of Z(Acc^6)$_4$O-*t*-Bu (Monoclinic and Triclinic Forms) and *p*-BrBz(Acc^6)$_4$O-*t*-Bu

donor	acceptor	symmetry operation	N···O distance, Å
		(a) Z(Acc^6)$_4$O-*t*-Bu (monoclinic form)	
N_3–H	O(2)	x, y, z	3.176
N_4–H	O_1	x, y, z	3.136
N_1–H	O_4	$x + 1, y, z$	2.990
		(b) Z(Acc^6)$_4$O-*t*-Bu (triclinic form)	
N_3–H	O(2)	x, y, z	3.184
N_4–H	O_1	x, y, z	3.067
N_1–H	O_4	$x, y, z + 1$	2.903
		(c) *p*-BrBz(Acc^6)$_4$O-*t*-Bu	
N_3–H	O(1)	x, y, z	3.135
N_4–H	O_1	x, y, z	3.006
N_1–H	O_3	$^1/_2 - x, -^1/_2 + y, ^3/_2 - z$	2.992
N_2–H	O_4	$^1/_2 - x, -^1/_2 + y, ^3/_2 - z$	3.148

The torsion angles of the *tert*-butyl ester group in all three structures show closely similar values, indicating staggering of the three methyls of the *tert*-butyl moiety about the C_4'–O_4* bond, as observed also in the *t*-Boc group.[50]

Cyclohexyl Ring Geometry and Conformation. The average bond angles, derived from a statistical analysis of the twelve Acc^6 residues discussed in this work, are strongly indicative of an asymmetric geometry at the C^α atom, as already found for the Aib residue.[51] All other endocyclic bond angles have values higher than those expected for a regular tetrahedral angle. The bond angles at the N and C′ atoms have values similar to those typical of a trans secondary peptide unit.[43,44]

As for the torsion angles relating the cyclohexyl ring to the peptide chain, N–C^α–$C^{\beta 1}$–$C^{\gamma 1}$ and N–C^α–$C^{\beta 2}$–$C^{\gamma 2}$ ($\chi^{1,1}$ and $\chi^{1,2}$), two sets of values are observed. In the former conformation (g^+, g^-; +60°, −60°) the α-amino group occupies the axial position, while in the latter (t, t; 180°, 180°) it is the α-carboxyl group that occupies the same position.[18] The (g^+,g^-) conformation is clearly predominant, in agreement with previous expectations.[1,18,23,24] Actually, only four (out of twelve) sets of (t, t) angles were found, three of which are in the structure of the *p*-BrBz-blocked homotetrapeptide.

The endocyclic torsion angles (θ_1–θ_6) are consistent with almost perfect chair conformations for the cyclohexyl ring of the Acc^6 side chains. These values should be compared with the expected torsion angles of ±54.7° in cyclohexane, with a C–C–C bond angle of 111.5°.[52] The total puckering amplitudes Q are also close to the Q value for an ideal cyclohexane chair (0.63 Å).[53]

Crystal Packing. A strong intermolecular N–H···O=C H bond between the urethane (or amide) N_1–H and the peptide O_4=C_4' groups of symmetry-related molecules characterizes the three structures. The N···O separations range from 2.903 to 2.992 Å. The other NH group, not involved in the intramolecular H-bonding scheme of the 3_{10} helices, is the peptide N_2H. In the crystal structure of the *p*-BrBz-blocked homotetrapeptide this donor is part of a weak intermolecular H bond with the O_3 atom as the acceptor (the pertinent N···O separation is 3.148 Å), whereas in the two crystalline forms of Z(Acc^6)$_4$O-*t*-Bu it is free. The average range of N···O separations observed for a large number of intermolecular N–H···O=C H bonds in peptides is 2.9–3.0 Å.[41,42] In the three structures packing is obtained through van der Waals interactions between

facing hydrophobic groups such as the methyl and the phenyl groups at the C- and N-terminals of the cyclohexyl moieties along the peptide chains as shown in Figures 6–8.

Conclusions

Homopeptides from Aib[2,3,45–47] and Acc[5 9] have been shown to strongly promote formation of 3_{10} helical structures. The present theoretical and experimental (X-ray diffraction) study is in favor of the conclusion that Acc[6] homopeptides also tend to assume such an ordered secondary structure. In view of the limited conformational space explorable by this residue, its homopolymer is, therefore, also expected to adopt the 3_{10} helical structure, as already reported for long, monodispersed homooligomers[3,54] and the polydispersed homopolymer[55] from Aib.

In addition, our previous findings on Acc[6] derivatives and small peptides[1,23,24] established that this $C^{\alpha,\alpha}$-dialkylated, cyclic residue can occur at either corner position ($i + 1$, $i + 2$) of type I (III) β-bends or at the $i + 2$ position of type II β-bends.[38–40] All these observations are useful when planning the synthesis of conformationally restricted analogues of bioactive peptides with folding at a predetermined sequence. Furthermore, this new residue has increased bulk and hydrophobicity compared to Aib and Acc[5] residues (having analogous conformational propensities). Finally, it is interesting to note that the homopeptides from the $C^{\alpha,\alpha}$-dialkylated *open-chain* analogues of Acc[6] (Deg[4] and Dpg[5]) exhibit significantly different structural tendencies (they favor the onset of fully extended, multiple C_5 forms[39]). This finding emphasizes the effect of the side-chain conformational change induced by cyclization on the preferred backbone structure.

Registry No. Ac-Acc[6]-NHMe, 103732-15-6; Z-$(Acc^6)_4$-OBu-*t*, 114273-55-1; *p*-BrBz-$(Acc^6)_4$-OBu-*t*, 114273-56-2.

References and Notes

(1) This work is part 177 of the series "Linear Oligopeptides". Part 176: Valle, G.; Crisma, M.; Toniolo, C.; Sen, N.; Sukumar, M.; Balaram, P. *J. Chem. Soc., Perkin Trans. 2*, in press.
(2) Benedetti, E.; Bavoso, A.; Di Blasio, B.; Pavone, V.; Pedone, C.; Crisma, M.; Bonora, G. M.; Toniolo, C. *J. Am. Chem. Soc.* **1982**, *104*, 2437.
(3) Toniolo, C.; Bonora, G. M.; Bavoso, A.; Benedetti, E.; Di Blasio, B.; Pavone, V.; Pedone, C. *Macromolecules* **1986**, *19*, 472.
(4) Smith, G. D.; Pletnev, V. Z.; Duax, W. L.; Balasubramanian, T. M.; Bosshard, H. E.; Czerwinski, E. W.; Kendrick, N. E.; Mathews, F. S.; Marshall, G. R. *J. Am. Chem. Soc.* **1981**, *103*, 1493.
(5) Ventakataram Prasad, B. V.; Balaram, P. *CRC Crit. Rev. Biochem.* **1984**, *16*, 307.
(6) Bosch, R.; Jung, G.; Schmitt, H.; Winter, W. *Biopolymers* **1985**, *24*, 961.
(7) Benedetti, E.; Barone, V.; Bavoso, A.; Di Blasio, B.; Lelj, F.; Pavone, V.; Pedone, C.; Bonora, G. M.; Toniolo, C.; Leplawy, M. T.; Kaczmarek, K.; Redlinsky, A. *Biopolymers*, in press.
(8) Benedetti, E.; Toniolo, C.; Hardy, P.; Barone, V.; Bavoso, A.; Di Blasio, B.; Grimaldi, P.; Lelj, F.; Pavone, V.; Pedone, C.; Bonora, G. M.; Lingham, I. *J. Am. Chem. Soc.* **1984**, *106*, 8146.
(9) Bardi, R.; Piazzesi, A. M.; Toniolo, C.; Sukumar, M.; Balaram, P. *Biopolymers* **1986**, *25*, 1635.
(10) Sukumar, M.; Raj, P. A.; Balaram, P.; Becker, E. L. *Biochem. Biophys. Res. Commun.* **1985**, *128*, 339.
(11) Tsang, J. W.; Schmied, B.; Nyfeler, R.; Goodman, M. *J. Med. Chem.* **1984**, *27*, 1663.
(12) Rodriguez, M.; Bland, J. M.; Tsang, J. W.; Goodman, M. *J. Med. Chem.* **1985**, *28*, 1527.
(13) Goodman, M. *Biopolymers* **1985**, *24*, 137.
(14) Park, W. K.; Choi, C.; Rioux, F.; Regoli, D. *Can. J. Biochem.* **1974**, *52*, 113.
(15) Hruby, V. J.; Kao, L. F.; Hirning, L. D.; Burks, T. F. In *Peptides: Structure and Function*; Deber, C. M., Hruby, V. J., Kopple, K. D., Eds.; Pierce Chemical Co.: Rockford, IL, 1985; pp 487–490.
(16) Kasafirek, E.; Vanzura, J.; Krejci, I.; Krepelka, J.; Dlabac, A.; Valchar, M. Belg. Patent BE 897 843, 1984; *Chem. Abstr.* **1984**, *100*, 192289d.
(17) MacDonald, R. N. U.S. Patent 2 572 843, 1951; *Chem. Abstr.* **1952**, *46*, 778g.
(18) Kenner, G. W.; Preston, J.; Sheppard, R. C. *J. Chem. Soc.* **1965**, 6239.
(19) Crisma, M.; Bonora, G. M.; Toniolo, C.; Bavoso, A.; Benedetti, E.; Di Blasio, B.; Pavone, V.; Pedone, C. *Macromolecules*, following paper in this issue.
(20) Benedetti, E.; Barone, V.; Bavoso, A.; Di Blasio, B.; Lelj, F.; Pavone, V.; Pedone, C.; Toniolo, C.; Crisma, M.; Bonora, G. M. In *Peptides 86*; Theodoropulos, D., Ed.; de Gruyter: Berlin, 1987; pp 315–318.
(21) Barone, V.; Benedetti, E.; Bavoso, A.; Di Blasio, B.; Lelj, F.; Pavone, V.; Pedone, C.; Toniolo, C.; Crisma, M.; Bonora, G. M. *Proc. Am. Pept. Symp., 10th* St. Louis, MO, 1987, in press.
(22) Chacko, K. K.; Srinivasan, R.; Zand, R. *J. Cryst. Mol. Struct.* **1971**, *1*, 261.
(23) Bardi, R.; Piazzesi, A. M.; Toniolo, C.; Sukumar, M.; Raj, P. A.; Balaram, P. *Int. J. Pept. Protein Res.* **1985**, *25*, 628.
(24) Paul, P. K. C.; Sukumar, M.; Bardi, R.; Piazzesi, A. M.; Valle, G.; Toniolo, C.; Balaram, P. *J. Am. Chem. Soc.* **1986**, *108*, 6363.
(25) Momany, F. A.; McGuire, R. F.; Burgess, A. W.; Scheraga, H. A. *J. Phys. Chem.* **1975**, *79*, 2361.
(26) Némethy, G.; Pottle, M. S.; Scheraga, H. A. *J. Phys. Chem.* **1983**, *87*, 1883.
(27) Zimmerman, S. S.; Pottle, M. S.; Némethy, G.; Scheraga, H. A. *Macromolecules* **1977**, *10*, 1.
(28) Lelj, F.; Barone, V., unpublished results.
(29) Davidon, W. C. *Comput. J.* **1968**, *10*, 406.
(30) Fletcher, R.; Powell, M. J. D. *Comput. J.* **1963**, *6*, 163.
(31) Harwell Library Routine No. VA11A.
(32) Germain, G.; Main, P.; Woolfson, M. M. *Acta Crystallogr., Sect. A* **1971**, *27*, 368.
(33) Cromer, D. T.; Waber, J. T. In *International Tables for X-Ray Crystallography*, 2nd Ed.; Kynoch: Birmingham, UK, 1974; Vol. 4, Table 2.2B.
(34) IUPAC-IUB Commission on Biochemical Nomenclature, *Biochemistry* **1970**, *9*, 3471.
(35) Donohue, J. *Proc. Natl. Acad. Sci. U.S.A.* **1953**, *39*, 470.
(36) Dickerson, R. E.; Geis, I. In *The Structure and Action of Proteins*; Harper and Row: New York, 1969.
(37) Richardson, J. S. *Adv. Protein Chem.* **1981**, *34*, 167.
(38) Venkatachalam, C. M. *Biopolymers* **1968**, *6*, 1425.
(39) Toniolo, C. *CRC Crit. Rev. Biochem.* **1980**, *9*, 1.
(40) Rose, G. D.; Gierasch, L. M., Smith, J. A. *Adv. Protein Chem.* **1985**, *37*, 1.
(41) Ramakrishnan, C.; Prasad, N. *Int. J. Protein Res.* **1971**, *3*, 209.
(42) Taylor, R.; Kennard, O.; Versikel, W. *Acta Crystallogr., Sect. B* **1984**, *40*, 280.
(43) Benedetti, E. In *Chemistry and Biochemistry of Amino Acids, Peptides and Proteins*; Weinstein, B., Ed.; Dekker: New York, 1982; Vol. 6, pp 105–184.
(44) Karle, I. L. In *The Peptides: Analysis, Structure, Biology*; Gross, E., Meienhofer, J., Eds.; Academic: New York, 1981; Vol. IV, pp 1–54.
(45) Toniolo, C.; Valle, G.; Bonora, G. M.; Crisma, M.; Formaggio, F.; Bavoso, A.; Benedetti, E.; Di Blasio, B.; Pavone, V.; Pedone, C. *Biopolymers* **1986**, *25*, 2237.
(46) Shamala, N.; Nagaraj, R.; Balaram, P. *J. Chem. Soc., Chem. Commun.* **1978**, 996.
(47) Pulla Rao, C.; Shamala, N.; Nagaraj, R.; Rao, C. N. R.; Balaram, P. *Biochem. Biophys. Res. Commun.* **1981**, *103*, 898.
(48) Benedetti, E.; Pedone, C.; Toniolo, C.; Dudek, M.; Némethy, G.; Scheraga, H. A. *Int. J. Pept. Protein Res.* **1983**, *21*, 163.
(49) Benedetti, E.; Ciajolo, A.; Di Blasio, B.; Pavone, V.; Pedone, C.; Toniolo, C.; Bonora, G. M. *Int. J. Pept. Protein Res.* **1979**, *14*, 130.
(50) Benedetti, E.; Pedone, C.; Toniolo, C.; Némethy, G.; Pottle, M. S.; Scheraga, H. A. *Int. J. Pept. Protein Res.* **1980**, *16*, 156.
(51) Paterson, Y.; Rumsey, S. M.; Benedetti, E.; Némethy, G.; Scheraga, H. A. *J. Am. Chem. Soc.* **1981**, *103*, 2947.
(52) Bixon, M.; Lifson, S. *Tetrahedron* **1967**, *23*, 769.
(53) Cromer, D.; Pople, J. A. *J. Am. Chem. Soc.* **1975**, *97*, 1354.
(54) Toniolo, C.; Bonora, G. M.; Barone, V.; Bavoso, A.; Benedetti, E.; Di Blasio, B.; Grimaldi, P.; Lelj, F.; Pavone, V.; Pedone, C. *Macromolecules* **1985**, *18*, 895.
(55) Malcolm, B. R.; Walkinshaw, M. D. *Biopolymers* **1986**, *25*, 607.